Published in final edited form as:
Life Sci. 2009 March 27; 84(13-14): 468–481. doi:10.1016/j.lfs.2009.01.014.

Apoptotic signaling induced by H_2O_2-mediated oxidative stress in differentiated C2C12 myotubes

Parco M. Siu[a,*], **Yan Wang**[b], and **Stephen E. Alway**[b]

[a] Department of Health Technology and Informatics, The Hong Kong Polytechnic University, Hung Hom, Kowloon, Hong Kong, China

[b] Laboratory of Muscle Biology and Sarcopenia, Division of Exercise Physiology, West Virginia University School of Medicine, Morgantown, West Virginia 26506, USA

Abstract

Aims: Apoptotic signaling proteins were evaluated in postmitotic skeletal myotubes to test the hypothesis that oxidative stress induced by H_2O_2 activates both caspase-dependent and caspase-independent apoptotic proteins in differentiated C2C12 myotubes. We hypothesized that oxidative stress would decrease anti-apoptotic protein levels in C2C12 myotubes.

Main methods: Apoptotic regulatory factors and apoptosis-associated proteins including Bcl-2, Bax, Apaf-1, XIAP, ARC, cleaved PARP, p53, $p21^{Cip1/Waf1}$, c-Myc, HSP70, CuZnSOD, and MnSOD protein content were measured by immunoblots.

Key findings: H_2O_2 induced apoptosis in myotubes as shown by DNA laddering and an elevation of apoptotic DNA fragmentation. Cell death ELISA showed increase in the extent of apoptotic DNA fragmentation following treatment with H_2O_2. Treatment with 4 mM of H_2O_2 for 24 or 96 h caused increase in Bax (56%, 227%), cytochrome *c* (282%, 701%), Smac/DIABLO (155%, 260%), caspase-3 protease activity (51%, 141%), and nuclear and cytosolic p53 (719%, 1581%) levels in the myotubes. As an estimate of the mitochondrial AIF release to the cytosol, AIF protein content measured in the mitochondria-free cytosolic fraction was elevated by 65% after 96 h treatment with 4 mM of H_2O_2. AIF measured in the nuclear protein fraction increased by 74% and 352% following treatment with 4 mM of H_2O_2 for 24 and 96 h, respectively. Bcl-2 declined in myotubes by 61% and 69% after 24 or 96 h of treatment in 4 mM H_2O_2, respectively.

Significance: These findings indicate that both caspase-dependent and caspase-independent mechanisms are involved in coordinating the activation of apoptosis induced by H_2O_2 in differentiated myotubes.

Keywords

Skeletal muscle; Oxidative stress; Apoptotic signaling; Programmed cell death

Introduction

Oxidative stress is defined when the production of reactive oxidants exceeds the cellular antioxidant capability. Substantial data have been assembled in exhibiting the essential role of oxidative stress in the regulation of diverse cellular events such as proliferation, differentiation, adhesion, oxidative damage and cell death (Droge 2002; Bergamini et al. 2004; Poli et al.

*Corresponding author. Tel.: +852 3400 8593; fax: +852 2362 4365. htpsiu@inet.polyu.edu.hk (P.M. Siu)..

2004; Martindale and Holbrook 2002; Simon et al. 2000). There is a growing body of evidence demonstrating a role of oxidative stress in the activation of apoptosis, which is an indispensable cellular process involved in governing cell survival/death during embryonic development, immunological defense, and tissue turnover (Anderson et al. 1999; Curtin et al. 2002; Fleury et al. 2002). Nonetheless, most investigations demonstrated oxidative stress and apoptosis in mitotic cell populations but little attention has been put on the role of oxidative stress in apoptosis in postmitotic muscle cells.

Aging is an unavoidable biological process that is typified by progressive loss of skeletal muscle mass and strength called sarcopenia. While the exact mechanisms that contribute to sarcopenia are largely unclear and still under active investigation, there has been recent evidence showing apoptosis is involved in the aging-associated loss of postmitotic tissues (i.e., skeletal and cardiac muscles and brain) because the occurrence of the pro-apoptotic events such as increases in Bax/Bcl-2, cytochrome *c* release, AIF, p53, caspases and/or DNA fragmentation in aged tissues (Alway et al. 2002, 2003a; Dirks and Leeuwenburgh 2002; Leeuwenburgh 2003; Phaneuf and Leeuwenburgh 2002; Pollack and Leeuwenburgh 2001; Pollack et al. 2002; Shelke and Leeuwenburgh 2003; Strasser et al. 2000; Woods et al. 2000; Alway and Siu 2008; Pistilli et al. 2006; Siu et al. 2005a; Siu et al. 2006). Base on the fact that apoptotic machinery can be initiated under redox control (Anderson et al. 1999; Curtin et al. 2002; Fleury et al. 2002) and concurrently, aging muscle has been shown to have elevated oxidative stress (Sastre et al. 2000; Sohal and Orr 1992), it is reasonable to hypothesize that the accelerated rate of apoptosis in aging muscle may be attributed to oxidative stress. There have been reports on muscle cell apoptosis (Liu and Ahearn 2001) but the causal role of oxidative stress in muscle apoptosis and the corresponding signaling mechanism have not been comprehensively examined.

Previously, there have been reports documenting the incidence of apoptosis under oxidative stress induced by H_2O_2 or menadione in proliferating skeletal myoblasts (Caporossi et al. 2003; Chiou et al. 2003; Stangel et al. 1996). However, the apoptotic consequences and the regulatory mechanisms responsible for the activation of the apoptotic program under oxidative stress are still poorly understood. Researchers investigating mitotic cells/tissues have identified a variety of elemental apoptotic molecules/proteins (e.g., BCL-2 family) crucial in mediating the signaling events leading to execution of apoptosis (Ellis et al. 1991; Danial and Korsmeyer 2004). Although apoptotic signal transduction in postmitotic skeletal muscle is poorly understood, there have been data showing that most of the apoptotic signaling components reported in single cell lineages are well-conserved in mature multinucleated skeletal muscle (Alway et al. 2002, 2003a; Dirks and Leeuwenburgh 2002; Dirks and Leeuwenburgh 2004; Ellis et al. 1991; McArdle et al. 1999; Pollack et al. 2002; Sandri et al. 1997; Sandri et al. 1998; Sandri et al. 2001; Tews 2002; Jin et al. 2001; Alway et al. 2003b; Siu et al. 2005b; Siu and Alway 2005). The aim of this study was to test the hypothesis that oxidative stress induced by H_2O_2 treatment in differentiated C2C12 myotubes would activate pro-apoptotic proteins and decrease anti-apoptotic proteins. As differentiated muscle cells are structurally (multinucleated), biochemically (expression of terminal myogenic proteins, e.g., myosin heavy chain), and functionally (contractile ability) different from proliferating myoblasts, in the present study we sought to examine differentiated skeletal myotubes as an in vitro model for mature developed but non-innervated skeletal muscle. The experiments were designed to examine both the dose- and time-dependent responses of apoptosis to H_2O_2 treatment.

Methods

Cell culture and treatment

Mouse-derived C2C12 myoblasts obtained from American Type Culture Collection (ATCC, Manassa, VA) were maintained in Dulbecco's modified Eagle's medium (DMEM)

supplemented with 10% fetal bovine serum, 100 U/ml penicillin G, 100 μg/ml streptomycin, and 0.25 μg/ml amphotericin fungizone, and incubated at 37 °C in a water-saturated atmosphere of 95% ambient air and 5% CO_2. Differentiated myotubes were prepared by culturing confluent C2C12 myoblasts in DMEM with 2% heat-inactivated horse serum and antibiotics (differentiation medium) to induce myogenic differentiation. In the present study, myotubes after 6 days of differentiation prepared on 100-mm culture plates were used as it has been shown that over 95% of C2C12 cultures are multinucleated myotubes following ~6-7 days of incubation in differentiation medium (Matsuki et al. 1999; McArdle et al. 1999). Fusion index as estimated by nuclei count in myotubes and myoblasts was determined to verify the proportional ratio of myotubes to myoblasts. C2C12 cells after 6 days of differentiation were grown on sterile glass cover slips, fixed in 4% paraformaldehyde in PBS (pH 7.4), and permeabilized with 0.1% Triton X-100 in 0.1% sodium citrate. The myotubes were incubated with anti-myosin heavy chain (MHC) antibody (MF20, Developmental Studies Hybridoma Bank, Iowa City, IA) followed by Cy3 conjugate $F(ab')_2$ fragment incubation (C2181, Sigma Chemical) to identify MHC in the fused myotubes. The nuclei were counterstained with DAPI using VECTA-SHIELD mounting medium (Vector Laboratories, Burlingame, CA). For the dose-dependent experiments, myotubes were treated with prepared dilutions of H_2O_2 in differentiation medium resulting in a final concentration of 1, 2, and 4 mM for 48 h. These doses were adopted base on the measurements on DNA fragmentation as determined by apoptotic cell death ELISA in myotubes in response to 48 h exposure to different doses (0, 0.2, 0.5, 1, 2 and 4 mM) of H_2O_2 (Fig. 1). Myotubes were also exposed to 4 mM of H_2O_2 for 24 and 96 h. Although 96 h is a relatively prolonged in vitro experimental situation, this time course permitted us to examine the time-dependent responses of myotubes to H_2O_2. Myotubes prepared from the same passage of myoblasts were treated with sterile water (i.e., vehicle of H_2O_2 dilution) and were included in the experiments of 24, 48, and 96 h treatment to act as the corresponding controls (i.e., 0 mM of H_2O_2). During the experiments, differentiation medium with H_2O_2 or sterile water was changed daily. The examinations on the myotubes were focused on the surviving cells and the floating cell debris which was removed during the change of medium were not included in the examinations in the present study.

Morphological imaging

Morphological changes and survival of cells were monitored by obtaining photomicrographs under an inverted phase contrast microscope (Olympus America Inc., Melville, NY) with a digital camera.

DNA gel electrophoresis laddering assay

Apoptotic DNA fragmentation was qualitatively analyzed by detecting the laddering pattern of nuclear DNA as described (Lu et al. 2002). Briefly, cells were harvested by scraping, washed in PBS, and lysed in 0.5 ml of DNA extraction buffer (50 mM Tris–HCl, 10 mM EDTA. 0.5% Triton, and 100 μg/ml proteinase K, pH 8.0) for overnight at 37 °C. The lysate was then incubated with 100 μg/ml DNase-free RNase A for 2 h at 37 °C, followed by three extractions of an equal volume of phenol/chloroform (1:1 v/v) and a subsequent re-extraction with chloroform by centrifuging at 15,000 rpm for 5 min at 4 °C. The extracted DNA was precipitated in 2 volume of ice-cold 100% ethanol with 1/10 volume of 3 M sodium acetate, pH 5.2 at −20 °C for 1 h, followed by centrifuging at 15,000 rpm for 15 min at 4 °C. After washing with 70% ethanol, the DNA pellet was air-dried and dissolved in 10 mM Tris–HCl/1 mM EDTA, pH 8.0. The DNA was then electrophoresed on 1.5% agarose gel and stained with ethidium bromide in Tris/acetate/EDTA (TAE) buffer (pH 8.5, 2 mM EDTA, and 40 mM Tris–acetate). A 100-bp DNA ladder (Invitrogen Life Technologies, Bethesda, MD) was included as a molecular size marker and DNA fragments were visualized and photographed by exposing the gels to ultraviolet transillumination.

Subcellular protein fractionation

The fractionation method described by Rothermel et al. (2000) was used to extract the cytosolic and nuclear protein fractions from C2C12 muscle cells with minor modification. In brief, cells were harvested by scraping in ice-cold lysis buffer (10 mM NaCl, 1.5 mM $MgCl_2$, 20 mM HEPES, pH 7.4, 20% glycerol, 0.1% Triton X-100, 1 mM dithiothreitol or DTT). Following centrifuging at 5000 rpm for 5 min at 4 °C to pellet the nuclei and cell debris, the supernatants were collected and these supernatants were further centrifuged three times at 5000 rpm for 5 min at 4 °C to remove residual nuclei and stored as nuclei-free total cytosolic protein fraction. A portion of this collected cytosolic extract (without addition of protease inhibitors) was stored and used later for fluorometric caspases-3 protease activity assay while a protease inhibitor cocktail containing 104 mM AEBSF, 0.08 mM aprotinin, 2 mM leupeptin, 4 mM bestatin, 1.5 mM pepstatin A, and 1.4 mM E-64 (Sigma-Aldrich, St Louis, MO) was added to the remaining portion. The cytosolic protein fraction with the addition of protease inhibitors was then used for cell death ELISA and Western immunoblots. The remaining nuclear pellets were then washed 3 times with ice-cold lysis buffer, resuspended in 240 μl of lysis buffer in the presence of 33.2 μl of 5 M NaCl and protease inhibitor cocktail, and rotated for 1 h at 4 °C to lyse the nuclei. Following a spin at 15,000 rpm for 15 min at 4 °C, the supernatants were collected and stored as cytosol-free nuclear protein fraction.

In order to estimate the release of mitochondria-housed apoptotic factors including cytochrome *c*, AIF, and Smac/DIABLO to the cytosol, a mitochondria-free cytosolic protein fraction was prepared as described by Rokhlin et al. (2002). Briefly, cells were scraped in ice-cold extraction buffer (250 mM sucrose, 20 mM HEPES, 10 mM KCl, 1.5 mM $MgCl_2$, 1 mM EDTA, 1 mM EGTA, 1 mM DTT, and 0.1 mM phenylmethylsulfonyl fluoride, pH 7.4) in the presence of protease inhibitor cocktail. Following a gentle homogenization with a Teflon pestle motorized with an electronic stirrer, homogenates were centrifuged at 800 ×g for 10 min at 4 °C to pellet the nuclei and cell debris. The supernatants were then spun twice at 16,000 ×g for 20 min at 4 °C to pellet the mitochondria and the final supernatants were collected as mitochondria-free cytosolic protein fractions. The purity of the protein fractions was confirmed by immunoblotting with an anti-histone H2B (a nuclear protein) rabbit polyclonal antibody (1:2000 dilution, 07371, Upstate, Lake Placid, NY), an anti-β-tubulin (a cytosolic cytoskeleton protein) rabbit polyclonal antibody (1:500 dilution, ab6046, Abcam, Cambridge, MA), an anti-SOD-1 or -CuZnSOD (a cytosolic isoform of superoxide dismutase) rabbit polyclonal antibody (1:500 dilution, sc-11407, Santa Cruz Biotechnology, Santa Cruz, CA), and an anti-MnSOD (a mitochondrial isoform of superoxide dismutase) goat antibody (1:2000 dilution, A300449A, Bethyl Lab, Montgomery, TX) (Fig. 2). The protein concentration of the protein extracts were quantified in duplicate by BCA Protein Assay (Pierce, Rockford, IL) based on the biuret reaction and the bicinchoninic acid detection of cuprous cation (Smith et al. 1985). As a further means to confirm the protein content, on a different occasion, all samples were then measured in duplicate by *DC* Protein Assay (BioRad, Hercules, CA) based on the reaction of protein with an alkaline copper tartrate solution and Folin reagent, which was similar to Lowry assay to confirm the protein contents (Lowry et al. 1951).

Apoptotic cell death ELISA

Cell death detection ELISA kit (Roche Applied Science, Indianapolis, IN) was used to quantitatively estimate the apoptotic DNA fragmentation by assessing the cytosolic histone-associated mono- and oligo-nucleosomes. In brief, the extracted nuclei-free cytosolic fraction was used as an antigen source in a sandwich ELISA with a primary anti-histone mouse monoclonal antibody coated to the microtiter plate and a second anti-DNA mouse monoclonal antibody coupled to peroxidase. The amount of peroxidase retained in the immunocomplex was determined photometrically by incubating with 2,2′-azino-di-[3-ethylbenzthiazoline sulfonate] (ABTS) as a substrate for 10 min at 20 °C. The change in color was measured at a

wavelength of 405 nm by using a Dynex MRX plate reader controlled through PC software (Revelation, Dynatech Laboratories, CA). Measurements were performed in duplicate with all samples analyzed on the same microtiter plate in the same setting. The OD_{405} reading was then normalized to the mg of protein used in the assay.

Identification of apoptotic nuclei in myotubes

To confirm the presence of DNA cleavage, which characteristically occurs in apoptotic cells, we identified apoptotic nuclei in myotubes in the presence or absence of H_2O_2. Apoptotic nuclei were examined by using a TdT-mediated dUTP nick-end labeling (TUNEL) assay (Roche Applied Science, Indianapolis, IN) after 24 h of 0, 1, 2 and 4 mM H_2O_2 treatments. Myotubes were grown on glass cover slips, fixed in 4% paraformaldehyde in PBS (pH 7.4), and permeabilized with 0.1% Triton X-100 in 0.1% sodium citrate. The cells were incubated with TdT and fluorescein-dUTP at 37 °C for 1 h. Myotubes were identified with anti-MHC antibody (MF20, Developmental Studies Hybridoma Bank, Iowa City, IA). Nuclei were counterstained with 4′,6-Diamidino-2-phenylindole (DAPI; Vectashield® mounting medium, Vector Laboratories, Burlingame, CA). The staining results were examined under a Nikon eclipse E800 fluorescence microscope and images were obtained and analyzed using a SPOT RT camera and SPOT RT software. The TUNEL-positive nuclei were counted with MHC-positive or MHC-negative staining to indicate TUNEL-positive nuclei in myotubes and myoblasts, respectively.

Fluorometric caspases-3 activity assay

Fifty microliter of the total cytosolic protein fraction without protease inhibitor was incubated in 50 μl of assay buffer (50 mM PIPES, 0.1 mM EDTA, 10% glycerol, 10 mM DTT, pH 7.2) with 100 μM of the fluorogenic 7-amino-4-trifluoromethyl coumarin (AFC)-conjugated substrate (Ac-DEVD-AFC, Alexis Corp., San Diego, CA) at 37 °C for 2 h. Caspase specific inhibitor, Z-VAD-FMK (Calbiochem, La Jolla, CA) was used as a control to validate the specificity of caspase. The change in fluorescence was measured on a spectrofluorometer with an excitation wavelength of 390/20 nm and an emission wavelength of 530/25 nm (CytoFluor, Applied Biosystems, Foster City, CA) before and after the 2 h incubation. Caspase activity was estimated as the change in arbitrary fluorescence units normalized to milligram protein used in the assay. Measurements were performed in duplicate while all the measurements were run on the same microplate in the same setting.

Immunoblot analyses

Protein expression of Bcl-2 (B-cell leukemia/lymphoma-2), Bax (Bcl-2-associated X protein), apoptosis protease activating factor-1 (Apaf-1), X-linked inhibitor of apoptosis (XIAP), apoptosis repressor with caspase recruitment domain (ARC), heat shock protein-70 (HSP70), and superoxide dismutases (CuZn- and Mn-SOD) was determined in the total cytosolic protein fraction. The protein content of apoptosis inducing factor (AIF), $p21^{Cip1/Waf1}$, c-Myc, and cleaved poly (ADP-ribose) polymerase (PARP) was measured in the nuclear fraction while p53 protein content was measured in both total cytosolic and nuclear fractions. Fifteen micrograms of protein was boiled at 95 °C for 5 min in Laemmli buffer and was separated by SDS-PAGE on 12% polyacrylamide gel. The gels were blotted to nitrocellulose membranes (VWR, West Chester, PA) and stained with Ponceau S red (Sigma Chemical Co, St Louis, MO) to verify equal loading and transferring of proteins to the membrane in each lane. As another approach to validate similar loading between the lanes, gels were loaded in duplicate with one gel stained with Coomassie blue. The membranes were then blocked in 5% non-fat milk in phosphate buffered saline with 0.05% Tween 20 (PBS-T) at room temperature for 1 h and probed with the following primary antibodies diluted in PBS-T with 2% BSA: anti-Bcl-2 mouse monoclonal antibody (1:100 dilution, sc-7382), anti-Bax rabbit polyclonal antibody

(1:200 dilution, sc-6236), anti-Apaf-1 rabbit polyclonal antibody (1:200 dilution, 3018, BioVision, Mountain View, CA), anti-hILP/XIAP mouse monoclonal antibody (1:250 dilution, 610762), anti-HSP70 mouse monoclonal antibody (1:2000 dilution, SPA810, StressGen, Victoria, BC, Canada), anti-SOD-1 rabbit polyclonal antibody (1:500 dilution, sc-11407), anti-MnSOD goat antibody (1:2000 dilution, A300449A, Bethyl Lab, Montgomery, TX), anti-AIF mouse monoclonal antibody (1:800 dilution, sc-13116HRP), anti-ARC rabbit polyclonal antibody (1:200 dilution, sc-11435), anti-cleaved PARP rabbit polyclonal antibody (1:1000 dilution, G734, Promega, Madison, WI), anti-p53 mouse monoclonal antibody (1:100 dilution, sc-99), anti-p21$^{Cip1/Waf1}$mouse monoclonal antibody (1:100 dilution, sc-550827), or anti-c-Myc mouse monoclonal antibody (1:200 dilution, 3800-1). Bcl-2, Bax, SOD-1, AIF, ARC, and p53 antibodies were purchased from Santa Cruz Biotechnology (Santa Cruz, CA) while XIAP, p21$^{Cip1/Waf1}$, and c-Myc antibodies were purchased from BD Biosciences (San Jose, CA). All primary antibody incubations were performed overnight at 4 °C. Secondary antibodies were conjugated to horseradish peroxidase (Chemicon International, Temecula, CA), and signals were developed by ECL detection kit (Amersham Biosciences, Piscataway, NJ). The signals were then visualized by exposing the membranes to X-ray films (BioMax MS-1, Eastman Kodak, Rochester, NY), and digital records of the films were captured with a Kodak 290 camera. Resulting bands were quantified as optical density (OD) × band area by an image analysis system (Eastman Kodak, Rochester, NY) and recorded in arbitrary units. The molecular sizes of the immunodetected proteins were verified by using pre-stained standard (LC5925, Invitrogen Life Technologies, Bethesda, MD).

Estimation of mitochondrial cytochrome c, Smac/DIABLO, and AIF release

Cytochrome *c*, AIF, and Smac/DIABLO (second mitochondria-derived activator of caspase) are apoptotic factors normally housed inside the mitochondria and their release to the cytosol has been demonstrated during the activation of apoptosis (Chang and Yang 2000). In this study, the release of Smac/DIABLO and AIF into the cytosol was estimated in the extracted mitochondria-free cytosolic protein fraction by immunoblotting with an anti-Smac/DIABLO mouse monoclonal antibody (1:500 dilution, 612244, BD Biosciences, San Jose, CA) and an anti-AIF monoclonal mouse antibody (1:800 dilution, sc-13116HRP). Moreover, a cytochrome *c* ELISA kit (MBL International, Woburn, MA) was used to assess the protein content of cytochrome *c* in the mitochondria-free cytosol fraction to evaluate the release of the mitochondrial cytochrome *c* to the cytosol. According to the manufacturer's protocol, 50 μl the extracted mitochondria-free cytosolic fraction was used as an antigen source in a sandwich ELISA with a horseradish peroxidase-conjugated anti-cytochrome *c* polyclonal antibody in microwell strips coated with an anti-cytochrome *c* antibody. After washing, the peroxidase retained in the immunocomplex was detected by incubating with a chromogenic substrate, tetramethylbenzidine/hydrogen peroxide (TMB/ H_2O_2) followed by adding an acid solution to terminate the enzyme reaction and to stabilize the developed color. The change in color was monitored at a wavelength of 450 nm using a Dynex MRX plate reader. Measurements were performed in duplicate with all the samples analyzed on the same microplate and the cytochrome *c* content was expressed as OD_{450} per mg protein.

Statistical analyses

All experiments were repeated on four different occasions (N=4). The data are expressed as percent relative to the control of the same occasion (i.e., 0 mM treatment represents 100% of control apoptotic expression levels) in order to designate the experimental change when comparing to the control condition. Results are given as means±standard error of mean (SE). Statistical analyses were performed using the SPSS 10.0 software package and one-way ANOVA with Tukey HSD post hoc test was used to examine the percent change in treatment relative to control. Multivariate analysis of variance (MANOVA) was performed on the percent changes in all measured variables in this study in order to examine the main effects of time,

dose, and interaction (time×dose). Estimate of the effect size by computing Eta squared (η^2, ranges from 0 to 1) was included in the MANOVA to designate how much of the total variance in our experiments was explained by the main effects or interaction. Statistical significance was accepted at $P<0.05$.

Results

Cell morphology

The maturity of differentiation of C2C12 myotubes was indicated by the expression of sarcomeric myosins (Fig. 3A). The fusion index as estimated by nuclei count in myotubes and myoblasts following MHC labeling was ~80% indicating a high proportional ratio of myotubes to myoblasts in our differentiated C2C12 culture. In addition, spontaneous contractile activity (i.e., twitching of elongated C2C12 myotubes) was occasionally observed in the C2C12 myotubes used in our experiments, suggesting that they had reached functional maturity. The morphological changes of C2C12 myotubes following a range of H_2O_2 treatment for 24, 48, or 96 h was monitored by an inverted phase contrast microscope. Fig. 3B shows that the morphological health condition and survival of cells was apparently reduced with increasing dose of H_2O_2 treatment or with a longer period of treatment. Myotubes were observed to become increasingly shrunk in cell volume with the H_2O_2 treatment suggesting atrophy.

Indicators of apoptosis: DNA laddering and cell death ELISA

DNA laddering gel electrophoresis is a suggested tool in detecting apoptosis in a highly specific manner as endonucleases cleave genomic DNA between the nucleosomes resulting in mono- and oligo-nucleosomes of ~200 base pairs or multiples during execution of apoptosis (Cain et al. 1994). In the present study, apoptotic DNA fragmentation was qualitatively examined using DNA laddering assay. The laddering pattern was absent in all extracted DNA from the control experiments (i.e., 0 mM of H_2O_2). Following 48 h exposure to 2 mM and 4 mM of H_2O_2 and 96 h exposure to 4 mM of H_2O_2, laddering pattern was clearly present in the extracted DNA (Fig. 4A). According to the results of our quantitative cell death ELISA, the extent of apoptotic DNA fragmentation following 24 h treatment with 4 mM of H_2O_2 was increased by 27% relative to 0 mM (Fig. 4B). After 48 h exposure to 2 mM and 4 mM of H_2O_2, the apoptotic DNA fragmentation was elevated by 37% and 99%, respectively while it was increased by 135% following 4 mM of H_2O_2 treatment for 96 h (Fig. 4B). The TUNEL/MHC labeling indicated that the apoptotic nuclei were predominately came from MHC-positively labeled C2C12 cells (i.e., differentiated myotubes) in response to H_2O_2 treatment (Fig. 4C).

BCL-2 family: Bcl-2 and Bax

In our immunoblots, we detected an immunoreactive band of ~25 kDa corresponding to the predicted molecular mass of Bcl-2 protein and a ~21 kDa immunoreactive band corresponding to Bax protein. We found that there was a 31% and 61% decrease in the Bcl-2 protein content following 48 h treatment with 2 mM and 4 mM of H_2O_2, respectively (Fig. 5A). After 96 h exposure to 4 mM of H_2O_2, Bcl-2 protein content was reduced by 69% (Fig. 5A). For the Bax protein content, there was a 56% increase after 24 h treatment with 4 mM of H_2O_2 (Fig. 5B). Following 48 h treatment with 2 mM and 4 mM of H_2O_2, we found that the Bax protein content was elevated by 108% and 122%, respectively while it was increased by 227% after 96 h treatment with 4 mM of H_2O_2 (Fig. 5B). The ratio of Bax/Bcl-2 protein content was calculated based on the results of Western analyses. There was a 567% and 1142% increase in the ratio of Bax/Bcl-2 following exposure to 4 mM of H_2O_2 for 48 h and 96 h, respectively (Fig. 5C).

Mitochondrial cytochrome c release and Apaf-1 content

The ELISA results using samples from the mitochondria-free cytosolic protein fraction demonstrated that the protein content of cytosolic cytochrome *c* increased by 282% following 24 h treatment with 4 mM of H_2O_2 (Fig. 6). After 48 h treatment with 2 mM and 4 mM of H_2O_2, the cytochrome c was elevated by 442% and 701%, correspondingly while it was increased by 701% after 96 h treatment with 4 mM of H_2O_2 (Fig. 6). In contrast, we did not find any difference in the cytosolic protein content of Apaf-1 following H_2O_2 exposures when compared to control ($P>0.05$, data not shown).

Caspase-3 protease activity

The protease activity of caspase-3, as determined by a fluorometric caspase activity analysis, was increased by 37% and 51% after 48 h exposure to 2 mM and 4 mM of H_2O_2, respectively (Fig. 7). There was a 141% elevation of caspase-3 activity following 96 h treatment with 4 mM of H_2O_2 (Fig. 7).

XIAP and ARC protein contents and mitochondrial Smac/DIABLO release

An immunoreactive band of ~57 and ~25 kDa corresponding to the predicted molecular mass of XIAP and ARC protein, respectively, was detected in the immunoblots of the total cytosolic fractions. The XIAP protein content was increased by 31% following 96 h treatment with 4 mM of H_2O_2 (Fig. 8A). For the ARC protein content, there was a 38% and 42% decrease after exposure to 4 mM of H_2O_2 for 48 h and 96 h, correspondingly (Fig. 8B). For the immunoblots of the extracted mitochondria-free cytosolic fractions, we detected an ~22 kDa immunoreactive band corresponding to the predicted molecular mass of the Smac/DIABLO protein. We found that the Smac/DIABLO protein content was upregulated by 115% after 24 h treatment with 4 mM of H_2O_2 (Fig. 8C). Following 48 h exposure to 1 mM, 2 mM, and 4 mM of H_2O_2, there was a 118%, 117%, and 260% increase in the Smac/DIABLO protein content, respectively (Fig. 8C). The Smac/DIABLO protein content was elevated by 466% after 96 h treatment with 4 mM of H_2O_2 (Fig. 8C).

Caspase-independent apoptotic events: mitochondrial AIF release and nuclear translocation

Translocation of mitochondrial AIF to the nuclei has been suggested to be a caspase-independent apoptotic event (Cande et al. 2002; Joza et al. 2001). As an estimate of the mitochondrial AIF release to the cytosol, the AIF protein content measured in the mitochondria-free cytosolic fraction was elevated by 65% after 96 h treatment with 4 mM of H_2O_2 (Fig. 9A). As assessed by immunoblots of nuclear protein fraction, we found that the nuclear AIF was increased by 174% and 352% following exposure to 4 mM of H_2O_2 for 48 h and 96 h, respectively (Fig. 9B).

Cleavage of protein substrate: cleaved PARP protein

PARP functions in the process of DNA repair and it has been shown to be a cleavage target for the effector caspase-3 during the execution of apoptosis (Lazebnik et al. 1994). According to our Western analysis, a ~85 kDa immunoreactive band corresponding to the cleaved PARP product was detected in the nuclear protein fraction extracted from the cells after 48 h and 96 h treatment with 4 mM of H_2O_2 (Fig. 10).

Cellular regulatory factors: p53, $p21^{Cip1/Waf1}$, and c-Myc protein contents

In our immunoblot analyses, an immunoreactive band of ~53 kDa corresponding to the predicted molecular mass of p53 protein was detected in the nuclear and the cytosolic protein fractions. There was a 719%, 909%, and 1581% increase in the nuclear p53 protein content after exposure to 4 mM of H_2O_2 for 24 h, 48 h, and 96 h, respectively (Fig. 11A). The cytosolic

p53 protein content was elevated by 71%, 93%, and 227% following treatment with 4 mM of H_2O_2 for 24 h, 48 h, and 96 h, correspondingly (Fig. 11B). On the contrary, we did not find any changes in the protein content of $p21^{Cip1/Waf1}$ and c-Myc following the H_2O_2 treatments as defined by ~21 kDa and 62 kDa immunoreactive bands, respectively, that were not different between the H_2O_2-treated and control cells ($P>0.05$, data not shown).

Heat shock stress protein and antioxidant enzyme: HSP70, MnSOD, and CuZnSOD protein contents

According to our immunoblot analyses, the protein content of HSP70, a stress protein, was increased by 131%, 103%, and 392% after exposure to 4 mM of H_2O_2 for 24 h, 48 h, and 96 h, respectively (Fig. 12A). For the antioxidant enzyme SOD, MnSOD protein content was increased by 23% following 96 h treatment with 4 mM of H_2O_2 (Fig. 12B) whereas there was no significant change in CuZnSOD protein content following H_2O_2 treatments ($P>0.05$, Fig. 12C).

Main effect of dose, time, and dose × time

The analysis of the multivariate tests in MANOVA examining all the measured variables showed that there were significant main effects of dose [$F(45, 36)=13.30$, $P<0.001$, $\eta^2=0.943$], time [$F(30, 22)=393.58$, $P<0.001$, $\eta^2=0.998$], and interaction (dose × time) [$F(30, 22)=393.58$, $P<0.001$, $\eta^2=0.998$] in explaining the variances of the present findings.

Discussion

Recent findings supported that apoptosis might have a regulatory role in age-related muscle loss (Alway et al. 2003a; Dirks and Leeuwenburgh 2002; Dirks and Leeuwenburgh 2004; Leeuwenburgh 2003; Pollack et al. 2002; Siu et al. 2005b). Since oxidative stress is elevated in aging muscle (Sastre et al. 2000; Sohal and Orr 1992) and apoptosis can be regulated under redox control (Hampton and Orrenius 1998; Ueda et al. 2002; Martindale and Holbrook 2002; Simon et al. 2000), oxidative stress-induced apoptosis has been hypothesized to be involved, at least in part, in muscle loss with aging. Indeed, there have been preliminary but limited in vitro data support the causal role of oxidative stress in muscle loss. The incidence of apoptosis has been previously documented in proliferating skeletal myoblasts, but not in postmitotic/differentiated skeletal muscle cells, in response to H_2O_2 or menadione (Caporossi et al. 2003; Chiou et al. 2003; Stangel et al. 1996). In the present study, we have confirmed the execution of apoptosis in postmitotic skeletal muscle cells under H_2O_2 induced oxidative stress and have identified changes in expression levels of several proteins involved in apoptotic signaling. We report apoptotic DNA fragmentation (evidence of apoptosis), elevation in pro-apoptotic Bax, decline in anti-apoptotic Bcl-2, increase in Bax/Bcl-2 relative ratio, mitochondrial release of cytochrome c, Smac/DIABLO and AIF, increase in caspase-3 protease activity, down-regulation of ARC, cleavage of PARP, and upregulation of p53 in differentiated C2C12 myotubes following H_2O_2 exposure.

Execution of apoptosis in postmitotic skeletal muscle cell under oxidative stress

There is a scarcity of data addressing the relationship between oxidative stress and apoptosis in postmitotic cells or tissues. Particularly, in skeletal muscle, the apoptotic consequence resulting from oxidative stress has not been fully defined. Although a few studies have attempted to examine the effect of oxidative stress on apoptosis in skeletal lineage muscle cells, all of these studies were conducted in muscle precursor cells (i.e., proliferating myoblasts) instead of differentiated and more functionally-mature muscle cells (i.e., postmitotic myotubes or myocytes) which are lacking the ability for proliferation after exiting the mitotic cell cycle (Caporossi et al. 2003; Chiou et al. 2003; Stangel et al. 1996). Stangel et al. (1996) first investigated the potential of skeletal myoblasts obtained from rat thigh muscle to undergo

apoptosis when exposed to H_2O_2, hypoxanthine/xanthine oxidase, and S-nitroso-N-acetylpenicillamine. By using a combination of different techniques including morphological examination, DNA laddering gel electrophoresis, and fluorescence activated cell sorting (FACS)-mediated molecular labeling for DNA strand breaks (in situ tailing and nick translation assay), they showed both H_2O_2 and NO induce apoptosis in a dose-dependent manner. Although the underlying mechanisms responsible for the execution of apoptosis were not examined in this study, more importantly, these findings clearly demonstrated that apoptotic cell death is fully operable in proliferating cells from myogenic origin (i.e., myoblasts) when exposed to H_2O_2 or NO. Subsequently, the observation of the activation of apoptosis in proliferating skeletal myoblasts under oxidative stress was further established (Caporossi et al. 2003; Chiou et al. 2003), in which insights on the signaling mechanisms were preliminarily revealed. Caporossi et al. (2003) showed that, in L6C5 rat myoblasts, apoptosis was evident when exposed to oxidative stress generated by moderate or high intensity of H_2O_2 based on the finding of increase in fragmented/condensed nuclei. They also found that the protease activity of caspase-3 was elevated, suggesting that caspase-dependent pathway was involved in explaining the activation of apoptosis. By using the technique of flow cytometry, Chiou et al. (2003) also demonstrated that caspases-3 was activated concomitant with increased hypodiploid cells and phosphatidylserine translocation in C2C12 mouse myoblasts in response to menadione (a reactive oxygen intermediate-generating chemical). On the contrary, in postmitotic/differentiated muscle, the effect of oxidative stress on apoptosis is relatively unknown. Differentiated muscle cells have been shown to preserve the capability for executing apoptosis when exposed to a classic apoptogenic agent staurosporine (a protein kinase inhibitor known to cause apoptosis in various cell types) (McArdle et al. 1999). Differentiated myotubes have also been demonstrated to be responsive to anabolic steroid, stanozolol in activating apoptosis (bu-Shakra et al. 1997). bu-Shakra et al. (1997) showed that mouse C2 myotubes exhibited apoptosis-related morphologic changes including cytoplasmic shrinkage, nuclear condensation and membrane blebbing together with apoptotic DNA fragmentation as determined by TUNEL and agarose gel eletrophoresis following stanozolol treatment. In the current study we extend the knowledge of apoptosis in skeletal muscle by demonstrating that oxidative stress, as induced by H_2O_2, is another potent stimulus in activating apoptosis in postmitotic/differentiated skeletal muscle cells. It is worth noting that the presently reported results in differentiated myotubes may be possibly confounded if there were considerable amount of remaining myoblasts in the examined cell culture. However, our measurements revealed that most of the examined muscle cells (~80%) were fused myotubes and our TUNEL analysis indicated that the apoptotic nuclei were predominantly found in the differentiated myotubes rather than myoblasts. Thus we interpret that the confounding artifact from the undifferentiated myoblasts to the presently reported findings should be minimal, if any. In general, the present in vitro data confirm the causal effect of oxidative stress on apoptosis in postmitotic muscle cells and are consistent with the previous in vivo findings, which suggested that oxidative stress may have an important role in accelerating apoptosis in mature skeletal muscles with atrophic condition (Alway et al. 2003a; Dirks and Leeuwenburgh 2002; Dirks and Leeuwenburgh 2004; Leeuwenburgh 2003; Pollack and Leeuwenburgh 2001; Pollack et al. 2002; Siu et al. 2005b; Siu and Alway 2005).

In the present study, the activation of apoptosis and the corresponding apoptotic signaling was demonstrated in C2C12 myotubes after exposure to a relatively high dose range of H_2O_2 (i.e., 1 to 4 mM) and these examined dosages were determined according to the results of preliminary experiments. The possible reason that we did not observe considerable apoptosis in myotubes following the treatment of low dose of H_2O_2 (e.g., 200 μM) in our preliminary experiments might be related to the relatively high resistance of differentiated myotubes to apoptosis when compared to myoblasts muscle cells and/or associated with the length of experimental period. Notably, the interpretation of the occurrence of apoptosis in C2C12 myotubes during H_2O_2 exposure in the present study was concluded from the biochemical data comprising the

presence of DNA laddering pattern in the genomic DNA extracted from H_2O_2-treated myotubes and the elevation of cytosolic histone-associated mono- and oligonucleosomes but electron microscopy-mediated morphological evidences defining apoptosis was lacking. Although it is anticipated that biochemical changes are in accordance with morphological events as have been demonstrated in staurosporine-induced apoptosis in C2C12 myotubes (McArdle et al. 1999), it is a limitation that our results were not substantiated by electron microscopic examination and this did not allow us to delineate the responsible morphological mechanisms as well as to differentiate the other potential forms of cell death including apoptosis, necrosis, oncosis and apoptotic oncosis, which have been shown in H_2O_2-treated mouse terminal proximal straight tubule S_3 cells (Takeda et al. 1999), in our examined conditions. In regard to the physiologic role of apoptosis in muscle loss, there has been hypothesized, but not directly proved yet, that apoptosis might have a function associated with the removal of individual nuclei and/or the loss of whole myofiber. While these hypothesized biologic roles of apoptosis remain to be verified, the present results suggested that the demonstrated H_2O_2-induced apoptosis was accompanied by decline in the amount of surviving myotubes base on the gross morphological observations. Nonetheless, the data did not allow us to determine the exact contribution of the activated apoptosis to the loss of nuclei or the death of myotubes or both. Further studies are warranted to comprehensively investigate the precise relationship of apoptosis between nuclei loss and muscle cell death in the atrophic conditions.

Apoptotic signaling in skeletal muscle cell under oxidative stress

Another scope of this study was to understand the apoptotic signaling pathways that contributed to the activation of apoptosis induced by oxidative stress in postmitotic skeletal muscle cells. The roles of members of the BCL-2 family in apoptosis, including the pro-apoptotic member Bax and anti-apoptotic member Bcl-2 have been investigated. It is generally agreed that Bax and Bcl-2 serve to control the release of mitochondria-housed apoptotic factors (e.g., cytochrome *c*, AIF, and Smac/DIABLO) by monitoring the formation of outer mitochondrial membrane channel/pore (Burlacu 2003; Danial and Korsmeyer 2004; Sharpe et al. 2004). In C2C12 myotubes following H_2O_2 treatment, we found an increase in Bax and a decrease in Bcl-2 concomitant with an elevation of the release of mitochondrial cytochrome *c*, AIF and Smac/DIABLO. The caspase protease family constitutes another important component of the apoptotic machinery (Grutter 2000). We found that the protease activity of caspase-3 was elevated together with the evidence of cleaved PARP fragment (a cleavage product generated by active caspase-3 proteolytic action) in C2C12 myotubes after exposure to H_2O_2 and these findings are consistent with the caspase-3 data in ROS-treated skeletal myoblasts (Caporossi et al. 2003; Chiou et al. 2003). It is also worth noting that we found increased AIF protein content in both mitochondria-free cytosolic and nuclear protein fractions suggesting the occurrences of mitochondrial AIF release and AIF nuclear translocation in C2C12 myotubes following H_2O_2 treatment. These findings clearly indicated that both caspase-dependent and -independent mechanisms contribute to the activation of apoptosis in postmitotic muscle cells when exposed to H_2O_2.

Apoptotic suppressors including ARC and XIAP were examined after H_2O_2 exposure in the current study. As expected, we found that the ARC protein content was down-regulated in response to H_2O_2. However, surprisingly, we found an increase, rather than a decrease, in XIAP protein content following 96 h treatment with 4 mM of H_2O_2.We interpret this observation as an adaptive response of postmitotic muscle cells to severe levels of oxidative stress perhaps in an attempt to minimize apoptosis. In support of this interpretation, it has been demonstrated that XIAP was upregulated under certain apoptotic conditions (e.g., rat skeletal gastrocnemius muscle with aging, human osteoblastic cell after gravity unloading, and human muscle with mitochondrial encephalomyopathies) (Dirks and Leeuwenburgh 2004; Nakamura et al. 2003;

Ikezoe et al. 2002) while life-long caloric restriction (an anti-apoptotic intervention) reduces XIAP in rat gastrocnemius muscle (Dirks and Leeuwenburgh 2004). Tumor suppressor p53 has been suggested to be an important regulator in the apoptotic signal transduction. In nuclei, p53 has been demonstrated to mediate apoptosis by transcriptional-dependent process of which upregulates the mRNA expression of certain pro-apoptotic genes including Bax, NOXA and p53-upregulated modulator of apoptosis (PUMA) (Schuler and Green 2001). It has also been shown that p53 can directly mediate the apoptotic signaling via a transcription-independent mechanism, of which p53 can be translocated to mitochondria and thereby activates the cytosolic pro-apoptotic apoptotic factors such as Bax (Chipuk et al. 2004). Intriguingly, there has been demonstrated that the p53-associated activation of apoptosis is dependent on the level of intracellular oxidative stress (Johnson et al. 1996; Lotem et al.1996). In accordance with the suggested pro-apoptotic role of p53 which might be oxidative stress-related, we report here that both the nuclear and cytosolic p53 protein content increased concomitant with the elevation of pro-apoptotic factor Bax in the H_2O_2-treated C2C12 myotubes.

Conclusion

The present study demonstrated elevation of apoptotic DNA fragmentation accompanied with pro-apoptotic signaling orchestrated by increases in Bax, mitochondrial cytochrome *c*, Smac/DIABLO and AIF releases, caspases-3 protease activity, as well as decreases in Bcl-2 and ARC in differentiated skeletal muscle cell following H_2O_2 exposure. Moreover, H_2O_2-induced an increase in nuclear AIF protein content indicating that nuclear translocation of AIF, a caspase-independent apoptotic process, was involved. These findings together suggested that both caspase-dependent and caspase-independent mechanisms are involved in coordinating the activation of apoptosis induced by H_2O_2. Additionally, p53 was markedly elevated concomitant with the pro-apoptotic signaling suggesting that p53 may also contribute to H_2O_2-induced apoptosis. Our findings confirm the execution of apoptosis under oxidative stress in postmitotic skeletal muscle cells. Also, these data provide a comprehensive analysis of apoptotic signaling and further clarify the proteins responsible for the activation of apoptotic machinery that is induced by H_2O_2 in differentiated skeletal muscle cells.

Acknowledgments

We are grateful to Dr. William Wonderlin for providing access to the CytoFluor spectrofluorometer in his lab and to Jeffrey Altemus, for access to the inverted phase microscope in the Imaging Analysis Facility, Department of Neurobiology and Anatomy at West Virginia University School of Medicine. We also acknowledge Dr. Julie Martyn for offering technical help in obtaining the immunocytochemistry on myosin expression in C2C12 cells. This study was supported by NIH: NIA Grant R01 AG021530 (SE Alway) and The Hong Kong Polytechnic University Research Funds A-PH69, A-PA7N and G-U469 (PM Siu).

References

Alway SE, Siu PM. Nuclear apoptosis contributes to sarcopenia. Exercise and Sport Science Reviews 2008;36(2):51–57.

Alway SE, Degens H, Krishnamurthy G, Smith CA. Potential role for Id myogenic repressors in apoptosis and attenuation of hypertrophy in muscles of aged rats. American Journal of Physiology. Cell Physiology 2002;283(1):C66–C76. [PubMed: 12055074]

Alway SE, Degens H, Krishnamurthy G, Chaudhrai Aa. Denervation stimulates apoptosis but not Id2 expression in hindlimb muscles of aged rats. Journals of Gerontology A, Biological Sciences and Medical Sciences 2003;58(8):687–697.

Alway SE, Martyn JK, Ouyang J, Chaudhrai A, Murlasits ZSb. Id2 expression during apoptosis and satellite cell activation in unloaded and loaded quail skeletal muscles. American Journal of Physiology. Regulatory, Integrative, and Comparative Physiology 2003;284(2):R540–R549.

Anderson KM, Seed T, Ou D, Harris JE. Free radicals and reactive oxygen species in programmed cell death. Medical Hypotheses 1999;52(5):451–463. [PubMed: 10416954]

Bergamini CM, Gambetti S, Dondi A, Cervellati C. Oxygen, reactive oxygen species and tissue damage. Current Pharmaceutical Design 2004;10(14):1611–1626. [PubMed: 15134560]

Burlacu A. Regulation of apoptosis by Bcl-2 family proteins. Journal of Cellular and Molecular Medicine 2003;7(3):249–257. [PubMed: 14594549]

bu-Shakra S, Alhalabi MS, Nachtman FC, Schemidt RA, Brusilow WS. Anabolic steroids induce injury and apoptosis of differentiated skeletal muscle. Journal of Neuroscience Research 1997;47(2):186–197. [PubMed: 9008149]

Cain K, Inayat-Hussain SH, Kokileva L, Cohen GM. DNA cleavage in rat liver nuclei activated by Mg2 + or Ca2+ + Mg2+ is inhibited by a variety of structurally unrelated inhibitors. Biochememistry and Cell Biology 1994;72(11–12):631–638.

Cande C, Cohen I, Daugas E, Ravagnan L, Larochette N, Zamzami N, Kroemer G. Apoptosis-inducing factor (AIF): A novel caspase-independent death effector released from mitochondria. Biochimie 2002;84(2–3):215–222. [PubMed: 12022952]

Caporossi D, Ciafre SA, Pittaluga M, Savini I, Farace MG. Cellular responses to H(2)O(2) and bleomycin-induced oxidative stress in L6C5 rat myoblasts. Free Radical Biology and Medicine 2003;35(11):1355–1364. [PubMed: 14642383]

Chang HY, Yang X. Proteases for cell suicide: functions and regulation of caspases. Microbiology and Molecular Biology Reviews 2000;64(4):821–846. [PubMed: 11104820]

Chiou TJ, Chu ST, Tzeng WF. Protection of cells from menadione-induced apoptosis by inhibition of lipid peroxidation. Toxicology 2003;191(2–3):77–88. [PubMed: 12965111]

Chipuk JE, Kuwana T, Bouchier-Hayes L, Droin NM, Newmeyer DD, Schuler M, Green DR. Direct activation of Bax by p53 mediates mitochondrial membrane permeabilization and apoptosis. Science 2004;303(5660):1010–1014. [PubMed: 14963330]

Curtin JF, Donovan M, Cotter TG. Regulation and measurement of oxidative stress in apoptosis. Journal of Immunological Methods 2002;265(1–2):49–72. [PubMed: 12072178]

Danial NN, Korsmeyer SJ. Cell death: critical control points. Cell 2004;116(2):205–219. [PubMed: 14744432]

Dirks A, Leeuwenburgh C. Apoptosis in skeletal muscle with aging. American Journal of Physiology. Regulatory, Integrative, and Comparative Physiology 2002;282(2):R519–R527.

Dirks AJ, Leeuwenburgh C. Aging and lifelong calorie restriction result in adaptations of skeletal muscle apoptosis repressor, apoptosis-inducing factor, X-linked inhibitor of apoptosis, caspase-3, and caspase-12. Free Radical Biology and Medicine 2004;36(1):27–39. [PubMed: 14732288]

Droge W. Free radicals in the physiological control of cell function. Physiological Reviews 2002;82(1):47–95. [PubMed: 11773609]

Ellis RE, Yuan JY, Horvitz HR. Mechanisms and functions of cell death. Annual Review of Cell Biology 1991;7:663–698.

Fleury C, Mignotte B, Vayssiere JL. Mitochondrial reactive oxygen species in cell death signaling. Biochimie 2002;84(2–3):131–141. [PubMed: 12022944]

Grutter MG. Caspases: key players in programmed cell death. Current Opinion in Structural Biology 2000;10(6):649–655. [PubMed: 11114501]

Hampton MB, Orrenius S. Redox regulation of apoptotic cell death. Biofactors 1998;8(1–2):1–5. [PubMed: 9699000]

Ikezoe K, Nakagawa M, Yan C, Kira J, Goto Y, Nonaka I. Apoptosis is suspended in muscle of mitochondrial encephalomyopathies. Acta Neuropathologica (Berlin) 2002;103(6):531–540. [PubMed: 12012084]

Jin H, Wu Z, Tian T, Gu Y. Apoptosis in atrophic skeletal muscle induced by brachial plexus injury in rats. Journal of Trauma 2001;50(1):31–35. [PubMed: 11231666]

Johnson TM, Yu ZX, Ferrans VJ, Lowenstein RA, Finkel T. Reactive oxygen species are downstream mediators of p53-dependent apoptosis. Proceedings of the National Academy Sciences of the United States of America 1996;93(21):11848–11852.

Joza N, Susin SA, Daugas E, Stanford WL, Cho SK, Li CY, Sasaki T, Elia AJ, Cheng HY, Ravagnan L, Ferri KF, Zamzami N, Wakeham A, Hakem R, Yoshida H, Kong YY, Mak TW, Zuniga-Pflucker JC, Kroemer G, Penninger JM. Essential role of the mitochondrial apoptosis-inducing factor in programmed cell death. Nature 2001;410(6828):549–554. [PubMed: 11279485]

Lazebnik YA, Kaufmann SH, Desnoyers S, Poirier GG, Earnshaw WC. Cleavage of poly (ADP-ribose) polymerase by a proteinase with properties like ICE. Nature 1994;371(6495):346–347. [PubMed: 8090205]

Leeuwenburgh C. Role of apoptosis in sarcopenia. Journals of Gerontology A, Biological Sciences and Medical Sciences 2003;58(11):999–1001.

Liu CC, Ahearn JM. Apoptosis of skeletal muscle cells and the pathogenesis of myositis: A perspective. Current Rheumatology Reports 2001;3(4):325–333. [PubMed: 11470052]

Lotem J, Peled-Kamar M, Groner Y, Sachs L. Cellular oxidative stress and the control of apoptosis by wild-type p53, cytotoxic compounds, and cytokines. Proceedings of the National Academy Sciences of the United States of America 1996;93(17):9166–9171.

Lowry OH, Rosebrough NJ, Farr AL, Randall RJ. Protein measurement with the Folin phenol reagent. Journal of Biological Chemistry 1951;193(1):265–275. [PubMed: 14907713]

Lu T, Xu Y, Mericle MT, Mellgren RL. Participation of the conventional calpains in apoptosis. Biochimica et Biophysica Acta 2002;1590(1–3):16–26. [PubMed: 12063165]

Martindale JL, Holbrook NJ. Cellular response to oxidative stress: Signaling for suicide and survival. Journal of Cellular Physiology 2002;192(1):1–15. [PubMed: 12115731]

Matsuki N, Takanohashi A, Boffi FM, Inanami O, Kuwabara M, Ono K. Hydroxyl radical generation and lipid peroxidation in C2C12 myotube treated with iodoacetate and cyanide. Free Radical Research 1999;31(1):1–8. [PubMed: 10489115]

McArdle A, Maglara A, Appleton P, Watson AJ, Grierson I, Jackson MJ. Apoptosis in multinucleated skeletal muscle myotubes. Laboratory Investigation 1999;79(9):1069–1076. [PubMed: 10496525]

Nakamura H, Kumei Y, Morita S, Shimokawa H, Ohya K, Shinomiya K. Suppression of osteoblastic phenotypes and modulation of pro- and anti-apoptotic features in normal human osteoblastic cells under a vector-averaged gravity condition. Journal of Medical and Dental Sciences 2003;50(2):167–176. [PubMed: 12968638]

Phaneuf S, Leeuwenburgh C. Cytochrome *c* release from mitochondria in the aging heart: a possible mechanism for apoptosis with age. American Journal of Physiology. Regulatory, Integrative, and Comparative Physiology 2002;282(2):R423–R430.

Pistilli EE, Jackson JR, Alway SE. Death receptor-associated pro-apoptotic signaling in aged skeletal muscle. Apoptosis 2006;11(12):2115–2126. [PubMed: 17051337]

Poli G, Leonarduzzi G, Biasi F, Chiarpotto E. Oxidative stress and cell signalling. Current Medicinal Chemistry 2004;11(9):1163–1182. [PubMed: 15134513]

Pollack M, Leeuwenburgh C. Apoptosis and aging: Role of the mitochondria. Journals of Gerontology A, Biological Sciences and Medical Sciences 2001;56(11):B475–B482.

Pollack M, Phaneuf S, Dirks A, Leeuwenburgh C. The role of apoptosis in the normal aging brain, skeletal muscle, and heart. Annals of the New York Academy of Sciences 2002;959:93–107. [PubMed: 11976189]

Rokhlin OW, Glover RA, Taghiyev AF, Guseva NV, Seftor RE, Shyshynova I, Gudkov AV, Cohen MB. Bisindolylmaleimide IX facilitates tumor necrosis factor receptor family-mediated cell death and acts as an inhibitor of transcription. Journal of Biological Chemistry 2002;277(36):33213–33219. [PubMed: 12091392]

Rothermel B, Vega RB, Yang J, Wu H, Bassel-Duby R, Williams RS. A protein encoded within the Down syndrome critical region is enriched in striated muscles and inhibits calcineurin signaling. Journal of Biological Chemistry 2000;275(12):8719–8725. [PubMed: 10722714]

Sandri M, Podhorska-Okolow M, Geromel V, Rizzi C, Arslan P, Franceschi C, Carraro U. Exercise induces myonuclear ubiquitination and apoptosis in dystrophin-deficient muscle of mice. Journal of Neuropathology and Experimental Neurology 1997;56(1):45–57. [PubMed: 8990128]

Sandri M, Minetti C, Pedemonte M, Carraro U. Apoptotic myonuclei in human Duchenne muscular dystrophy. Laboratory Investigation 1998;78(8):1005–1016. [PubMed: 9714187]

Sandri M, El Meslemani AH, Sandri C, Schjerling P, Vissing K, Andersen JL, Rossini K, Carraro U, Angelini C. Caspase 3 expression correlates with skeletal muscle apoptosis in Duchenne and facioscapulo human muscular dystrophy. A potential target for pharmacological treatment? Journal of Neuropathology and Experimental Neurology 2001;60(3):302–312. [PubMed: 11245214]

Sastre J, Pallardo FV, Garcia dlA, Vina J. Mitochondria, oxidative stress and aging. Free Radical Research 2000;32(3):189–198. [PubMed: 10730818]

Schuler M, Green DR. Mechanisms of p53-dependent apoptosis. Biochemical Society Transactions 2001;29(Pt 6):684–688. [PubMed: 11709054]

Sharpe JC, Arnoult D, Youle RJ. Control of mitochondrial permeability by Bcl-2 family members. Biochimica Biophysica Acta 2004;1644(2–3):107–113.

Shelke RR, Leeuwenburgh C. Lifelong caloric restriction increases expression of apoptosis repressor with a caspase recruitment domain (ARC) in the brain. FASEB Journal 2003;17(3):494–496. [PubMed: 12514107]

Simon HU, Haj-Yehia A, Levi-Schaffer F. Role of reactive oxygen species (ROS) in apoptosis induction. Apoptosis 2000;5(5):415–418. [PubMed: 11256882]

Siu PM, Alway SE. Id2 and p53 participate in apoptosis during unloading-induced muscle atrophy. American Journal of Physiology. Cell Physiology 2005;288(5):1058–1073.

Siu PM, Pistilli EE, Alway SEa. Apoptotic responses to hindlimb suspension in gastrocnemius muscles from young adult and aged rats. American Journal of Physiology. Regulatory, Integrative, and Comparative Physiology 2005;289(4):R1015–R1026.

Siu PM, Pistilli EE, Butler DC, Alway SEb. Aging influences the cellular and molecular responses of apoptosis to skeletal muscle unloading. American Journal of Physiology. Cell Physiology 2005;288 (2):C338–C349. [PubMed: 15483226]

Siu PM, Pistilli EE, Murlasits Z, Alway SE. Hindlimb unloading increases muscle content of cytosolic but not nuclear Id2 and p53 proteins in young adult and aged rats. Journal of Applied Physiology 2006;100(3):907–916. [PubMed: 16282427]

Smith PK, Krohn RI, Hermanson GT, Mallia AK, Gartner FH, Provenzano MD, Fujimoto EK, Goeke NM, Olson BJ, Klenk DC. Measurement of protein using bicinchoninic acid. Analytical Biochemistry 1985;150(1):76–85. [PubMed: 3843705]

Sohal RS, Orr WC. Relationship between antioxidants, prooxidants, and the aging process. Annals of the New York Academy of Sciences 1992;663:74–84. [PubMed: 1482104]

Stangel M, Zettl UK, Mix E, Zielasek J, Toyka KV, Hartung HP, Gold R. H2O2 and nitric oxide-mediated oxidative stress induce apoptosis in rat skeletal muscle myoblasts. Journal of neuropathology and experimental neurology 1996;55(1):36–43. [PubMed: 8558170]

Strasser H, Tiefenthaler M, Steinlechner M, Eder I, Bartsch G, Konwalinka G. Age dependent apoptosis and loss of rhabdosphincter cells. Journal of Urology 2000;164(5):1781–1785. [PubMed: 11025769]

Takeda M, Shirato I, Kobayashi M, Endou H. Hydrogen peroxide induces necrosis, apoptosis, oncosis and apoptotic oncosis of mouse terminal proximal straight tubule cells. Nephron 1999;81(2):234–238. [PubMed: 9933761]

Tews DS. Apoptosis and muscle fibre loss in neuromuscular disorders. Neuromuscular Disorders 2002;12 (7–8):613–622. [PubMed: 12207928]

Ueda S, Masutani H, Nakamura H, Tanaka T, Ueno M, Yodoi J. Redox control of cell death. Antioxidants and Redox Signalling 2002;4(3):405–414.

Woods K, Marrone A, Smith J. Programmed cell death and senescence in skeletal muscle stem cells. Annals of the New York Academy of Sciences 2000;908:331–335. [PubMed: 10911979]

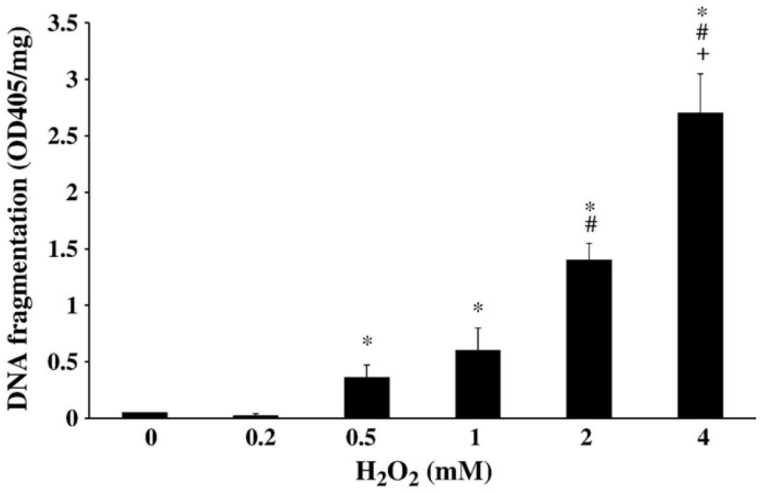

Fig. 1.

DNA fragmentation of myotubes in response to different doses of H_2O_2. DNA fragmentation was quantitatively examined by cell death ELISA in 6-day differentiated C2C12 myotubes treated with 0, 0.2, 0.5, 1, 2 and 4 mM of H_2O_2 for 48 h. **P*<0.05, data are significantly different from the corresponding 0 mM H_2O_2; **P*<0.05, data are significantly different from 1 mM H_2O_2; ^{+}P<0.05, data are significantly different from 2 mM H_2O_2.

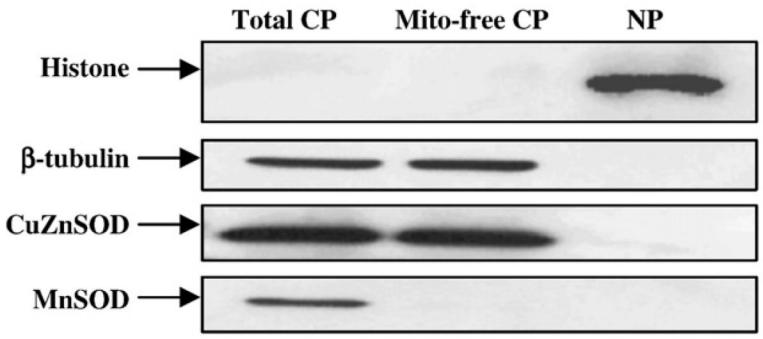

Fig. 2.

Verification of protein extract purity. The purity of protein fractions was verified by immunoblotting with anti-histone H2B, anti-β-tubulin, anti-CuZnSOD, and anti-MnSOD antibodies. An equal amount of total cytosolic (Total CP), mitochondria-free cytosolic (Mito-free CP), and nuclear (NP) protein was used in the immunoblot.

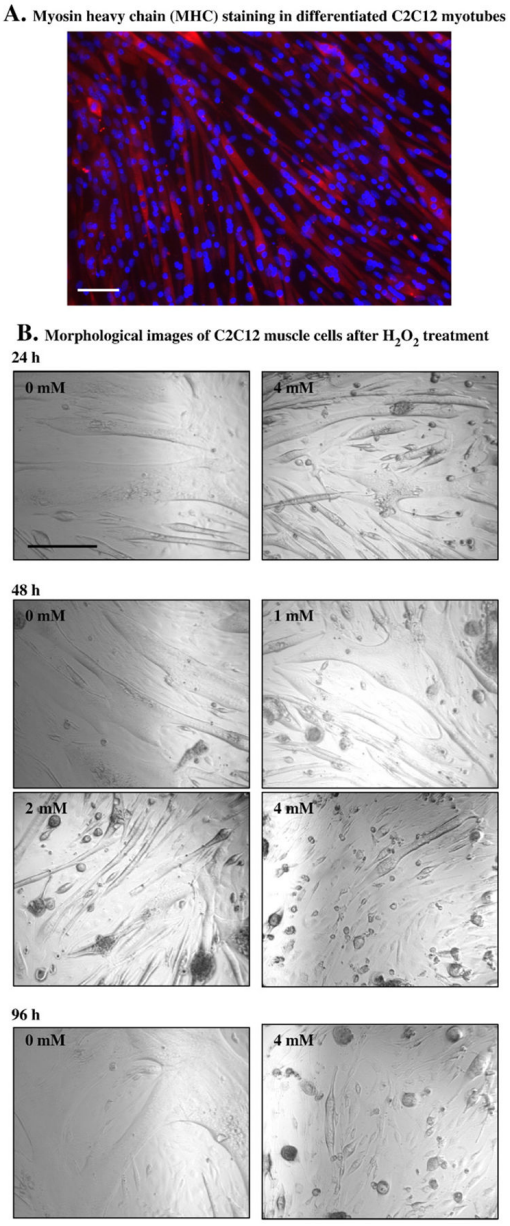

Fig. 3.

Morphology C2C12 Myotubes. (A). 6-day differentiated C2C12 myotubes were incubated with a mouse monoclonal MF20 antibody against sarcomeric myosin heavy chains (MF20, Developmental Studies Hybridoma Bank, University of Iowa, IA). Red fluorescence was developed by incubation with Cy3 following MF20 primary antibody incubation. Nuclei were counterstained with DAPI. These data show the high proportional ratio of myotubes to myoblasts in our used C2C12 culture. Objective, 20×. Bar, 100 μm. (B). The C2C12 myotubes were treated with 0, 1, 2, and 4 mM of H_2O_2 for 48 h and with 4 mM of H_2O_2 for 24 h and 96 h. The morphological health condition and survival of cells was apparently declined with increasing dose of H_2O_2 treatment or with prolonging period of treatment. Objective, 40×. Bar, 100 μm.

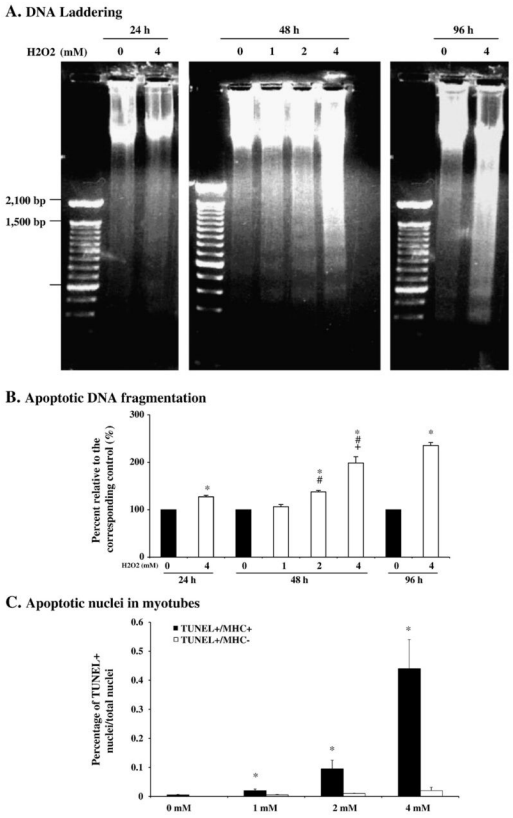

Fig. 4.

DNA laddering and apoptotic DNA fragmentation. Apoptotic DNA fragmentation was qualitatively analyzed by DNA gel electrophoresis (A). The extracted DNA was loaded on 1.5% agarose gel and was stained with ethidium bromide. The extent of apoptotic DNA fragmentation was quantitatively examined by measuring the cytosolic mono- and oligo-nucleosomes with ELISA (B). The data are presented as means±standard error of mean (SE) of percent relative to 0 mM H_2O_2 (i.e., 0 mM refers to 100% of the level of DNA fragmentation in control samples). *P<0.05, data are significantly different from the corresponding 0 mM H_2O_2; $^{\#}P$<0.05, data are significantly different from 1 mM H_2O_2; ^{+}P<0.05, data are significantly different from 2 mM H_2O_2. Quantitative data of TUNEL labeling in myotubes treated with H_2O_2 for 24 h (C). The staining results were analyzed under a Nikon eclipse E800 fluorescence microscope. For each of the four treatment groups (H_2O_2 0, 1, 2, 4 mM), 3 observation fields were randomly chosen. The following three parameters were counted: a) TUNEL-positive nuclei located within MHC-positive myotubes, b) TUNEL-positive nuclei located outside of MHC-positive myotubes, and c) total nuclei in each observation field were counted; the percentage of a/c and b/c was calculated. The data are presented as means ±standard deviation. * P<0.05, data are significantly different from the TUNEL-positive/ MHC-negative group.

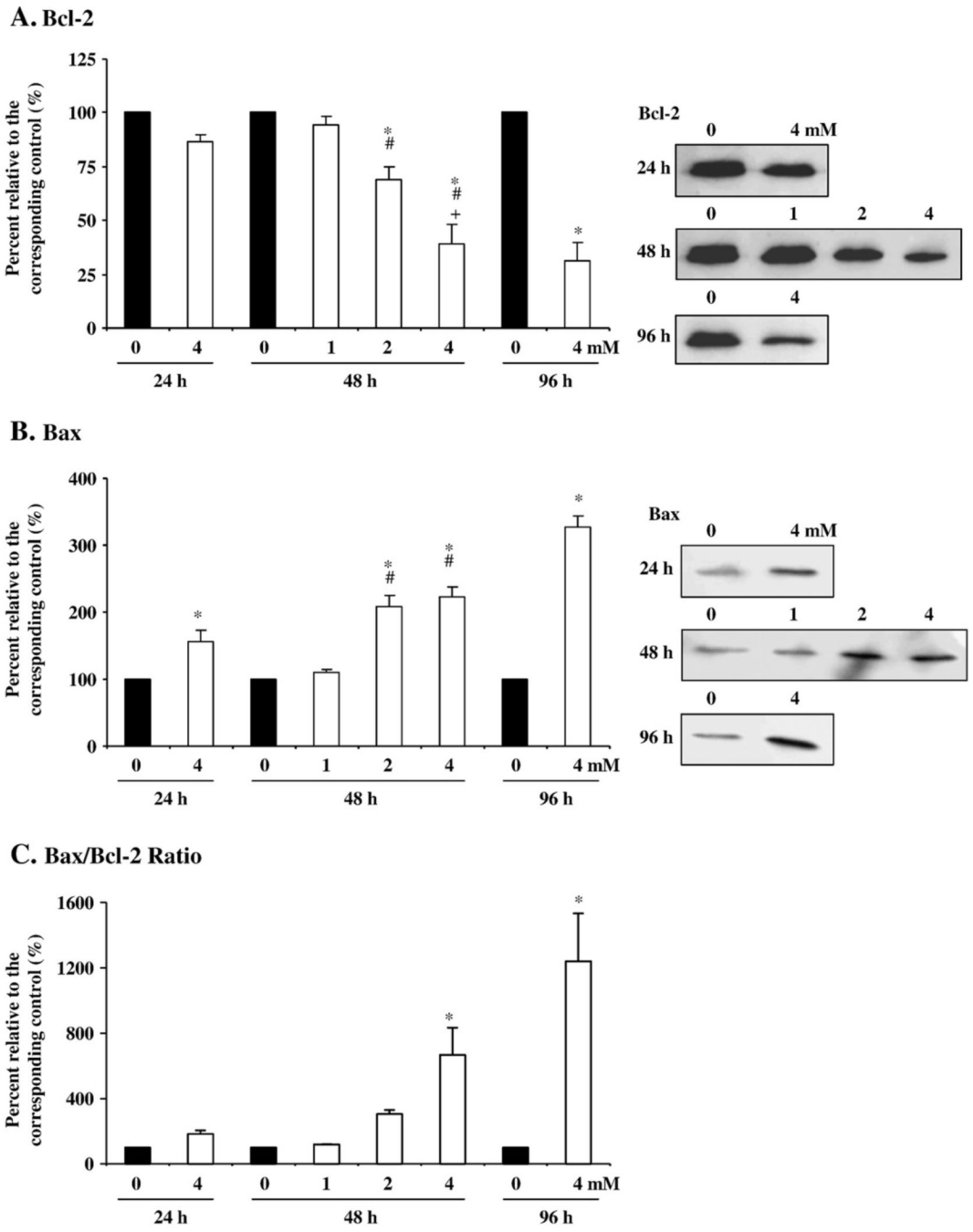

Fig. 5.

Bcl-2 and Bax. The protein content of Bcl-2 (A) and Bax (B) was determined by Western analysis. Insets show representative blots. The ratio of Bax/Bcl-2 protein content (C) was estimated according to the data of Western analysis. The data are presented as means±SE of percent relative to 0 mM H_2O_2 (i.e., 0 mM refers to 100% of the level of Bcl-2 and Bax protein content in control samples). *P<0.05, data are significantly different from the corresponding 0 mM H_2O_2; $^{\#}P$<0.05, data are significantly different from 1 mM; ^{+}P<0.05, data are significantly different from 2 mM H_2O_2.

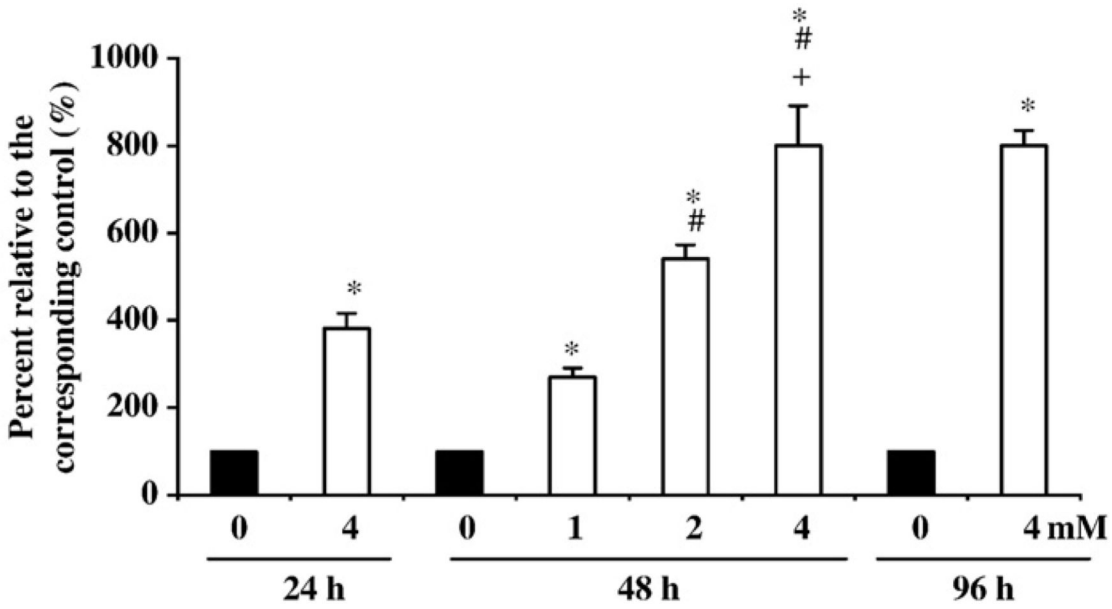

Fig. 6.

Mitochondrial cytochrome *c* release. The release of mitochondrial cytochrome *c* was estimated by examining the cytochrome *c* protein content in the extracted mitochondria-free cytosolic fraction with an ELISA. The data are presented as means±SE of percent relative to 0 mM H_2O_2 (i.e., 0 mM refers to 100% of the cytochrome *c* protein content in control samples). **P*<0.05, data are significantly different from the corresponding 0 mM H_2O_2; $^{\#}P$<0.05, data are significantly different from 1 mM; ^{+}P<0.05, data are significantly different from 2 mM H_2O_2.

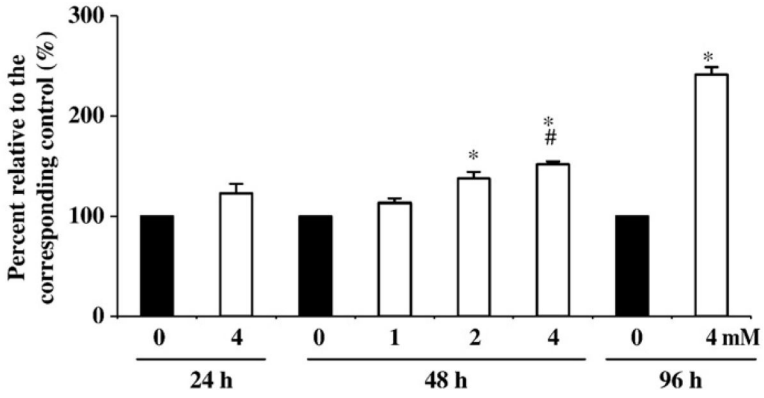

Fig. 7.

Caspase-3 protease activity. The change in fluorescence during a 2 h incubation of a fluorometric assay specific for caspase-3 protease activity is normalized to mg protein used in the assay. The normalized data are presented as mean±SE of percent relative to 0mMH_2O_2 (i.e., 0 mM refers to 100% of the level of caspase 3 protease activity in control samples). *P<0.05, data are significantly different from the corresponding 0 mM H_2O_2; $^{\#}P$<0.05, data are significantly different from 1 mM H_2O_2.

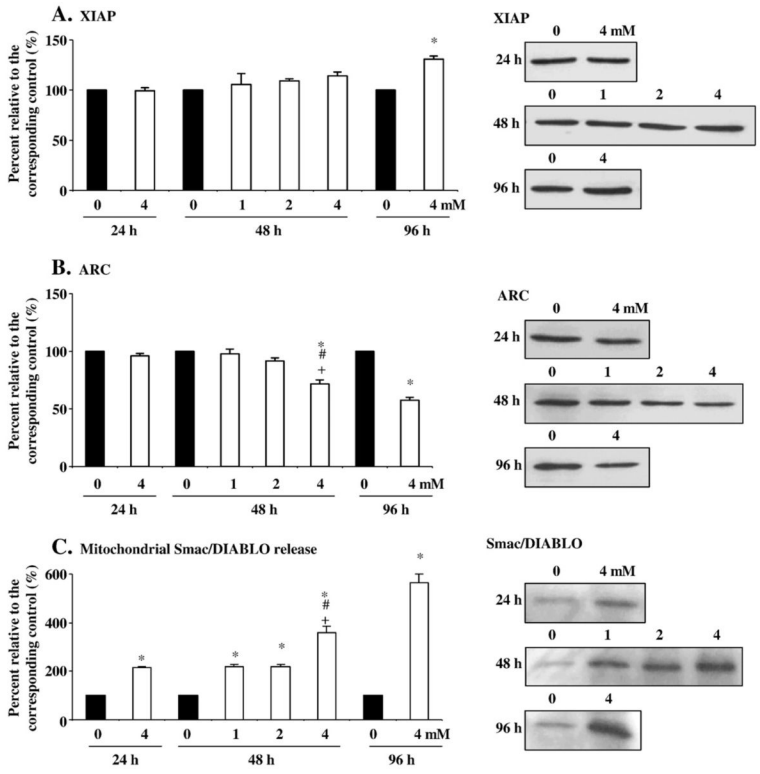

Fig. 8.

XIAP, ARC, and Smac/DIABLO protein. The protein content of XIAP (A), ARC (B), and Smac/DIABLO (C), was measured by Western immunoblot in the total cytosolic (XIAP and ARC) and mitochondria-free cytosolic fractions (Smac/DIABLO). The insets show representative blots. The data are presented as means±SE of percent relative to 0 mM H_2O_2 (i.e., 0 mM refers to 100% of the level of the respective protein content in control samples). *P<0.05, data are significantly different from the corresponding 0 mM; $^{\#}P$<0.05, data are significantly different from 1 mM H_2O_2; ^{+}P<0.05, data are significantly different from 2 mM H_2O_2.

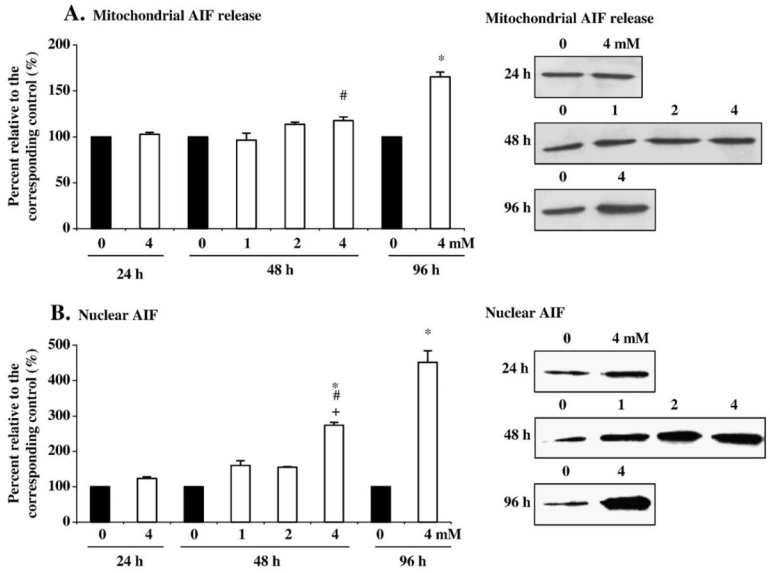

Fig. 9.

AIF protein. The AIF protein content was determined in mitochondria-free cytosolic (A) and nuclear protein fraction (B) by Western analysis in order to indicate the extent of mitochondrial release and nuclear translocation of AIF, correspondingly. The insets show representative blots. The data are presented as means±SE of percent relative to 0 mM of H_2O_2 (i.e., 0 mM refers to 100% of the level of AIF protein content in control samples). $^{*}P<0.05$, data are significantly different from the corresponding 0 mM H_2O_2; $^{\#}P<0.05$, data are significantly different from 1 mM; $^{+}P<0.05$, data are significantly different from 2 mM H_2O_2.

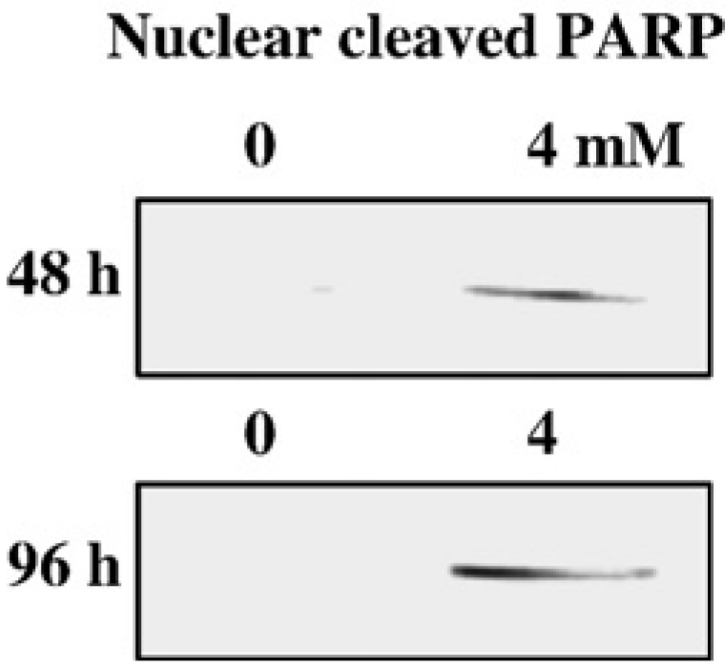

Fig. 10.
Cleaved PARP. The p85 cleaved PARP fragment was detected by Western immunoblot in the nuclear protein fraction obtained from cells followed 4 mM of H_2O_2 treatment for 48 h and 96 h.

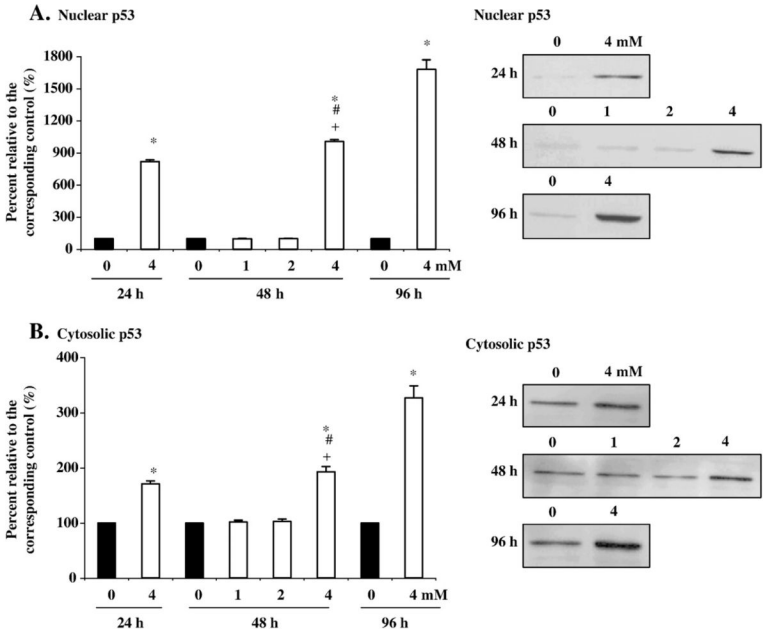

Fig. 11.

p53 protein. The p53 protein content was determined in nuclear (A) and total cytosolic protein fraction (B) by Western analysis. The insets show representative blots. The data are presented as means±SE of percent relative to 0 mM H_2O_2 (i.e., 0 mM refers to 100% of the level of p53 protein content in control samples). **P*<0.05, data are significantly different from the corresponding 0 mM H_2O_2; $^{\#}P$<0.05, data are significantly different from 1 mM H_2O_2; ^{+}P<0.05, data are significantly different from 2 mM H_2O_2.

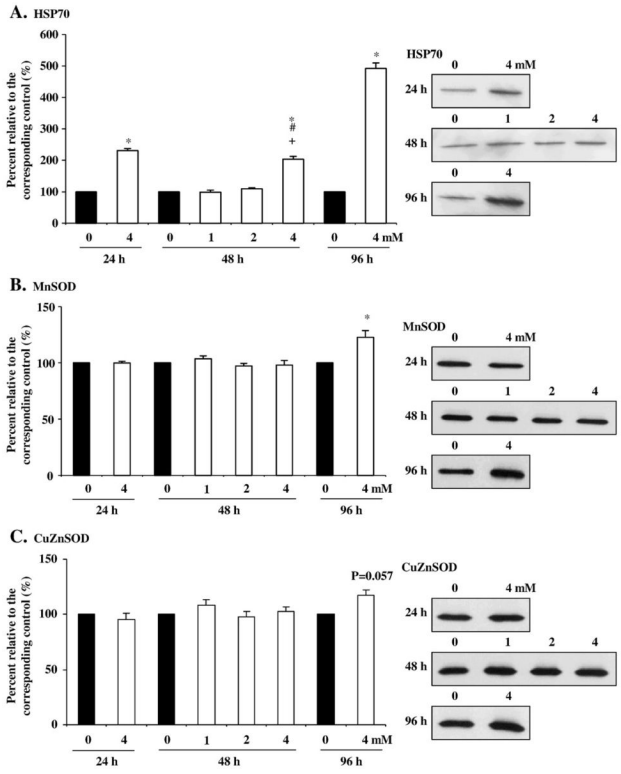

Fig. 12.

HSP70, MnSOD, and CuZnSOD protein. The protein content of HSP70 (A), MnSOD (B), and CuZnSOD (C) was determined in the total cytosolic fraction by Western immunoblot. The insets show representative blots. The data are presented as means±SE of percent relative to 0 mM H_2O_2 (i.e., 0 mM refers to 100% of the respective protein content level in control samples). *P<0.05, data are significantly different from the corresponding 0 mM; $^{\#}P$<0.05, data are significantly different from 1 mM H_2O_2; ^{+}P<0.05, data are significantly different from 2 mM H_2O_2.